Annals of Nuclear Medicine Vol. 13, No. 6, 427–431, 1999

Two cases of focal nodular hyperplasia of the liver: Value of scintigraphy with Tc-99m GSA and positron emission tomography with FDG

Susumu SHIOMI,* Hiroko KUROOKA,* Yoshinori IWATA,* Nobumitsu SASAKI,* Kyoko MASAKI,* Hisato JOMURA,* Shuhei NISHIGUCHI,* Tetsuo KUROKI* and Hironobu OCHI**

**Third Department of Internal Medicine and **Division of Nuclear Medicine, Osaka City University Medical School*

Focal nodular hyperplasia (FNH) of the liver is relatively rare, and can be difficult to differentiate from other benign tumors arising in the liver. We describe a 23-year-old woman and a 25-year-old man with FNH. They were hospitalized for further evaluation of a space-occupying lesion in the liver. Scintigraphy with Tc-99m diethylenetriaminepentaacetic acid galactosyl human serum albumin (Tc-99m GSA) revealed increased radioactivity in the tumor in one patient and radioactivity similar to that in the normal part of liver in the other. F-18 fluorodeoxyglucose positron emission tomography (FDG-PET) showed uptake similar to that of the normal liver in both patients. FNH was diagnosed on the basis of angiographic findings and histological findings in liver biopsy specimens. Our results show that scintigraphy with Tc-99m GSA and FDG-PET may provide information helpful in the diagnosis of FNH.

Key words: FDG, Tc-99m GSA, focal nodular hyperplasia, positron emission tomography

INTRODUCTION

FOCAL NODULAR HYPERPLASIA (FNH) is a benign hepatic tumor that characteristically occurs in women of reproductive age. It is often discovered incidentally.[1] Since both hepatic adenoma and hepatocellular carcinoma (HCC) require surgical treatment,[2] distinguishing FNH from these tumors is mandatory to avoid an unnecessary operation. To make a definite diagnosis of FNH, its characteristics must be confirmed by imaging studies. The characteristics of FNH have been described on the basis of various image techniques, including ultrasonography,[3,4] computed tomography (CT),[3,5] and magnetic resonance imaging (MRI)[6,7] but imaging studies do not always yield typical findings, and it is often difficult to make a definite diagnosis by such a method alone. Imaging with a radionuclide based on functional aspects of Kupffer cells and hepatocytes offers valuable information not available with other imaging techniques. Such information may be useful for the diagnosis of FNH. We report two cases of FNH in which scintigraphy with Tc-99m diethylenetriaminepentaacetic acid galactosyl human serum albumin (Tc-99m GSA) and positron emission tomography with F-18 fluorodeoxyglucose (FDG-PET) were performed.

Received June 23, 1999, revision accepted September 9, 1999.

For reprint contact: Susumu Shiomi, M.D., Third Department of Internal Medicine, Osaka City University Medical School, 1–4–3 Asahimachi, Abeno-ku, Osaka 545–8585, JAPAN.

E-mail: shiomis@med.osaka-cu.ac.jp

CASE REPORT

Case 1.

A 23-year-old woman was referred to our hospital because of left hypochondrium pain. Abdominal ultrasonography showed a space-occupying lesion in the liver, and the patient was hospitalized.

On admission, the patient was of moderate build and well-nourished. The red blood cell count was $495 \times 10^4/mm^3$, the platelet count was $9.5 \times 10^4/mm^3$, the serum albumin concentration was 4.7 g/dL, the aspartate transferase activity was 24 IU/L, the alanine aminotransferase activity was 24 IU/L, the cholinesterase activity was 575 IU/L, the total bilirubin concentration was 1.0 mg/dL, the α-fetoprotein concentration was 4 ng/mL, the carcinoembryonic antigen was 1.1 ng/ml, the hepatitis B surface antigen was negative, and the hepatitis C virus antibody was negative.

Contrast CT in the early phase revealed a tumor with uniform density in the liver (Fig. 1A); that in the late phase revealed an irregular high density area in the tumor (Fig. 1B). Color Doppler flow imaging showed a central color spot with a pulsatile wave in the mass (Fig. 2A). Celiac angiography showed a centrifugal vascular structure in the tumor (Fig. 2B). Scintigraphy with Tc-99m GSA revealed increased radioactivity in the tumor (Fig. 3A). FDG-PET showed uptake similar to that in the normal part of the liver (Fig. 3B). Hematoxylin-eosin staining of a specimen obtained by liver biopsy under ultrasonic guidance revealed no malignant lesion and extensive scar-like connective tissue, including abundant thick-walled arteries and proliferating bile ducts (Fig. 4).

Case 2.

A 25-year-old man was referred to our hospital because of abnormal results of liver blood tests. Abdominal ultrasonography showed a space-occupying lesion in the liver, and the patient was hospitalized.

On admission, the patient was of moderate build and well-nourished. The red blood cell count was $465 \times 10^4/mm^3$, the platelet count was $9.2 \times 10^4/mm^3$, the serum albumin concentration was 4.2 g/dL, the aspartate transferase activity was 46 IU/L, the alanine aminotransferase activity was 42 IU/L, the γ-glutamyl transpeptidase activity was 86 IU/L, the cholinesterase activity was 465 IU/L, the total bilirubin concentration was 0.8 mg/dL, the α-fetoprotein concentration was 3 ng/mL, the carcinoembryonic antigen was 1.0 ng/ml, the hepatitis B surface antigen was negative, and the hepatitis C virus antibody was negative.

CT angiography in the artery phase revealed a tumor with high density (Fig. 5A), and that in the venous phase revealed low density in the liver (Fig. 5B). Celiac angiography showed a centrifugal vascular structure in the tumor (Fig. 6). Scintigraphy with Tc-99m GSA revealed uptake similar to that in the normal part of the liver (Fig. 7A). FDG-PET also showed uptake similar to that in the normal part of the liver (Fig. 7B). Hematoxylin-eosin staining of a specimen obtained by liver biopsy under ultrasonic guidance revealed no malignant lesion and extensive scar-like connective tissue, including abundant thick-walled arteries and proliferating bile ducts (Fig. 8).

DISCUSSION

Pathologically, FNH consists of hepatocytes and Kupffer cells and shows normal hepatic architecture. It often has a thin fibrous capsule. A central satellite-shaped collagenous scar with peripherally radiating septae is a typical finding.[1,8] We used percutaneous fine-needle biopsy to confirm the diagnosis of FNH, but diagnosis may be difficult when a small biopsy specimen containing only normal hepatocytes is obtained, without the extensive scar-like connective tissue. Sampling errors may also occur.

A central stellate scar is considered pathognomonic of FNH. In our patients, CT showed a hypodense area in the center of the tumor, suggesting a central scar, but this feature is detected in only a limited number of cases, with a central stellate scar being visualized in 18% to 26% of patients by ultrasonography,[3,4] 14% to 61% by CT,[3,5] and 35% to 79% by MRI.[6,7] Another feature of FNH is its specific vascular architecture, in which a large tortuous artery enters the center of the tumor and then supplies the nodules centrifugally.[8] This anatomical feature appears as a wheel spike on angiograms and is unique to FNH. However, this feature was detected in only 44% of patients undergoing angiography.[9] In recent years, angio CT[10] and color Doppler ultrasonogrphy[4,11,12] have been developed to evaluate the hemodynamics of liver tumors in detail.

Normal or increased uptake of colloid scan has been suggested as pathognomonic of FNH, which contains functioning Kupffer cells.[9] This finding is useful in discriminating between FNH and hepatic adenoma since the latter, which lacks Kupffer cells, shows a focal defect on colloid scintigraphy.[13,14] Nevertheless, Welch et al.[3] reported that among 10 tumors studied with Tc-99m sulfur colloid, 4 (40%) had increased uptake as compared with the normal liver; 3 (30%) had uptake similar to that of the liver, and 3 (30%) had decreased uptake. Roger et al.[9] reported that 4 (36%) of 11 cases showed decreased uptake on scintigraphy with Tc-99m sulfur colloid.

Tc-99m GSA scintigraphy of the liver is based on visualization of the receptor binding of Tc-99m GSA to liver cells.[15] In general, the accumulation of Tc-99m GSA is related to the functional activity and the number of functioning hepatocytes. A localized area of decreased accumulation of Tc-99m GSA can be expected where a decreased number of asialoglycoprotein receptors are present. It is well known that the receptor-mediated binding with subsequent cellular endocytosis does not occur in HCC or metastatic tumors because surface asialoglycoprotein receptors are lost during malignant dedifferentiation.[16,17] But, Saito et al.[18] reported that scintigraphy with Tc-99m GSA showed increased uptake in 2 (25%) of 8 patients with well differentiated HCC because some well differentiated HCCs have asialoglycoprotein receptor.[19]

Kutaran et al.[20] reported that scintigraphy with Tc-99m GSA showed increased uptake in 8 (67%) of 12 patients and normal uptake in the remaining 4 (33%) and, thus, the method was useful for the diagnosis of FNH. One of our patients showed an increased uptake and the other, a normal uptake. Hepatic tumors seldom show an increased uptake on scintigraphy with Tc-99m GSA, and this finding is characteristic of FNH and well differentiated HCC. The

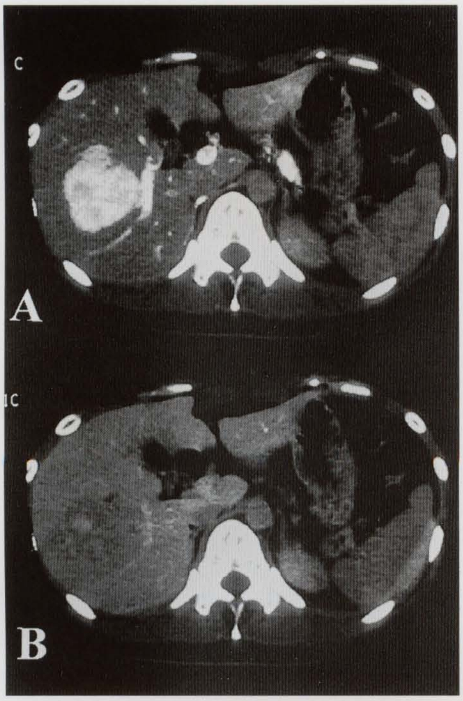

Fig. 1

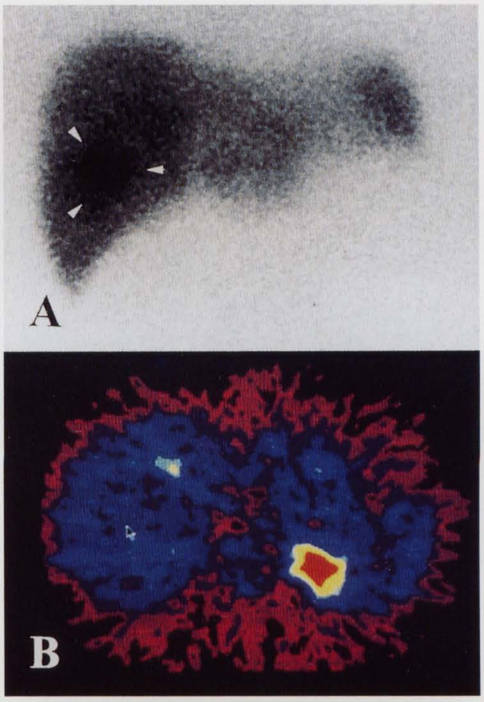

Fig. 3

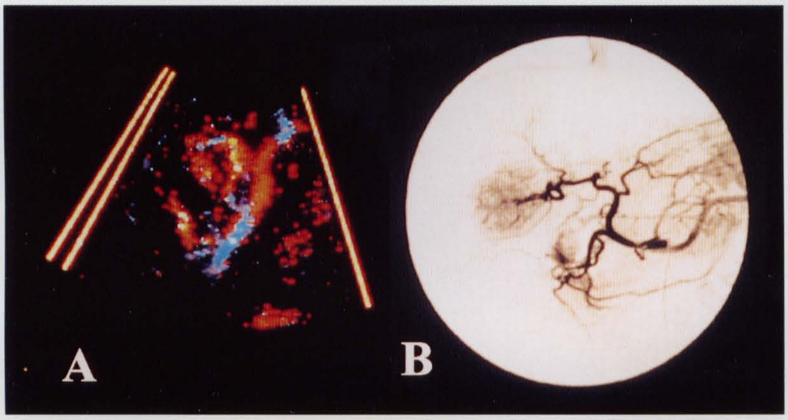

Fig. 2

Fig. 1 A. Contrast computed tomography (CT) in the early phase revealed a tumor with uniform density in the liver. B. Contrast CT in the late phase revealed an irregular high density area in the tumor.

Fig. 2 A. Color Doppler flow imaging showed a central color spot with a pulsatile wave in the mass. B. Celiac angiography showed a centrifugal vascular structure in the tumor.

Fig. 3 A. Scintigraphy with Tc-99m GSA revealed increased radioactivity in the tumor. B. FDG-PET showed uptake similar to that in the normal part of the liver.

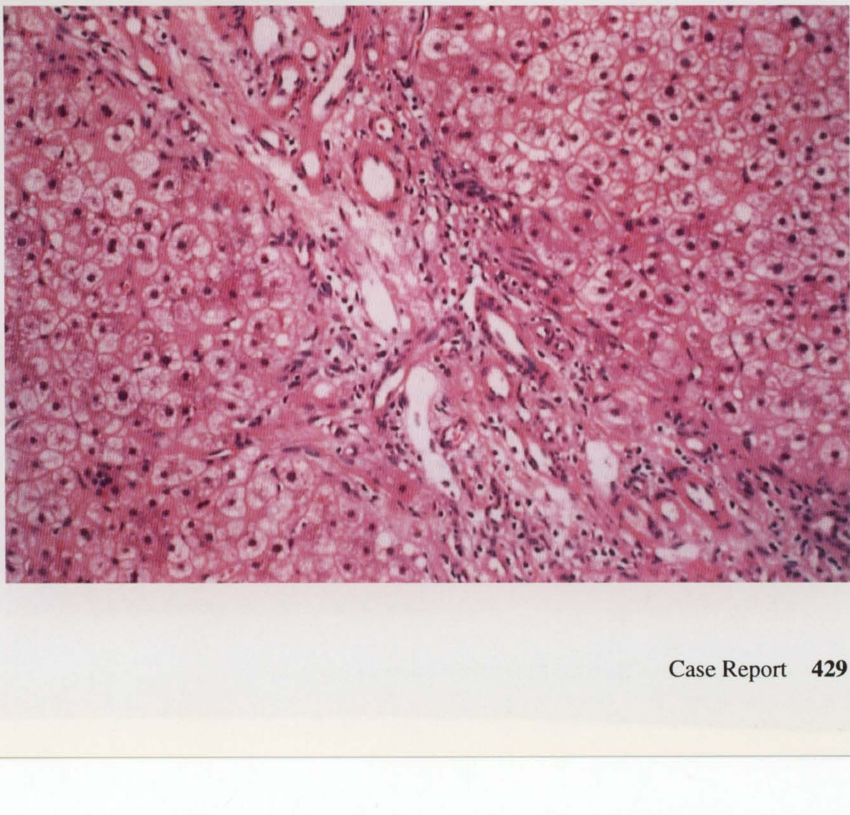

Fig. 4 Examination of a liver biopsy specimen revealed no malignant lesion and extensive scar-like connective tissue, including abundant thick-walled arteries and proliferating bile ducts (H&E, × 100).

Fig. 5 A. CT angiography in the arterial phase revealed a tumor with high density. B. CT angiography in the portal phase revealed low density in the tumor.

Fig. 6 Celiac angiography showed a centrifugal vascular structure in the tumor.

Fig. 7 A. Scintigraphy with Tc-99m GSA revealed uptake similar to that in the normal part of the liver. B. FDG-PET showed uptake similar to that in the normal part of the liver.

Fig. 5

Fig. 6

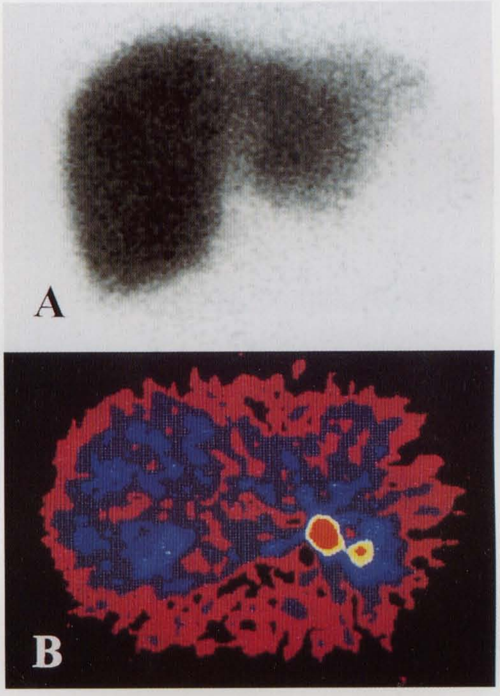

Fig. 7

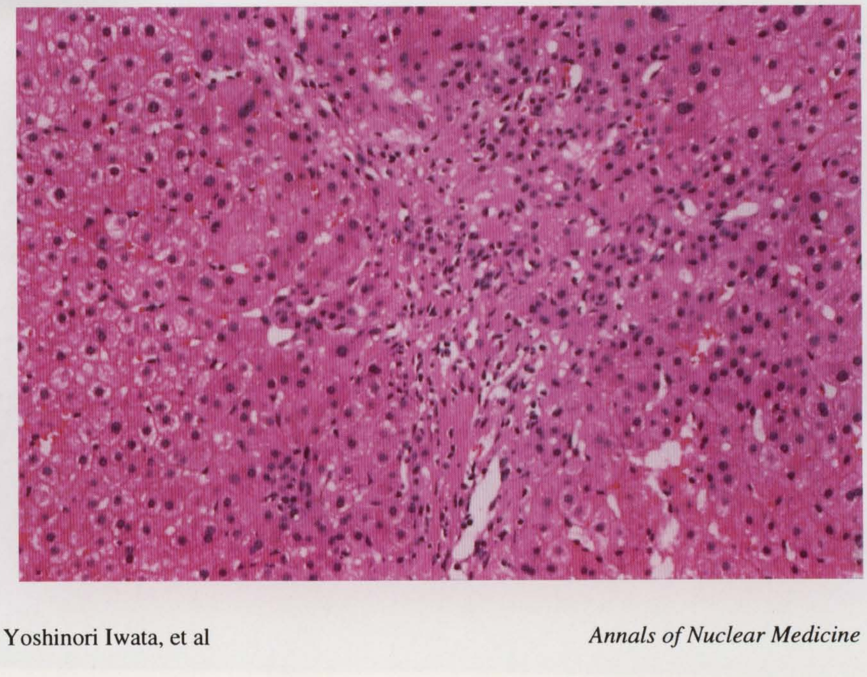

Fig. 8 Examination of a liver biopsy specimen revealed no malignant lesion and extensive scar-like connective tissue, including abundant thick-walled arteries and proliferating bile ducts (H&E, × 100).

increased uptake on scintigraphy is likely to be caused by an increase in cell density, but there was no increase in cell density in our two cases, and the cause of the increased uptake could not be determined.

We also performed FDG-PET in both cases. PET has been used recently to diagnose various types of tumors,[21] and FDG-PET is considered particularly useful in the diagnosis of HCC and cholangiocellular carcinoma.[22] Although the use of FDG-PET for the diagnosis of FNH has not been reported previously, the uptake was similar to that in the normal part of the liver in both of our patients. Torizuka et al.[23] reported that glucose metabolism as assessed by FDG-PET closely reflects the enzymatic activity of glucose. This shows that glucose metabolism in FNH does not differ from that in the normal liver despite the presence of hyperplasia.

In conclusion, imaging procedures such as ultrasonography, CT and MRI do not always yield typical finding, and it is often difficult to make a definite diagnosis of FNH by such a method alone. Our findings show that FDG-PET and scintigraphy with Tc-99m GSA may provide information helpful in the diagnosis of FNH.

REFERENCES

1. Edomondson HA, Peters RL. Tumors of the liver: pathologic features. *Semin Roentgenol* 18: 75–83, 1983.
2. Rooks JB, Ory HW, Ishak KG, Strauss LT, Greenspan JR, Hill AP, et al. Epidemiology of hepatocellular adenoma. The rule of oral contraceptive use. *JAMA* 242: 644–648, 1979.
3. Welch TJ, Sheedy PF, Johnson CM, Stephen DH, Charboneau JW, Brown ML, et al. Focal nodular hyperplasia and hepatic adenoma: comparison of angiography, CT, US, and scintigraphy. *Radiology* 156: 593–595, 1985.
4. Goli M, Mathieu D, Anglade M-C, Cherqui D, Vasile N, Rahmouni A, et al. Focal nodular hyperplasia of the liver: value of color Doppler US in association with MR imaging. *Radiology* 187: 113–117, 1993.
5. Belghiti J, Pateron D, Panis Y, Vilgrain V, Flejou JF, Benhamou JP, et al. Resection of presumed benign liver tumors. *Br J Surg* 80: 380–383, 1993.
6. Rummeny E, Weissleder R, Sironi S, Stark DD, Comptom CC, Hahn PF, et al. Central scars in primary liver tumors: MR features, specificity, and pathologic correlation. *Radiology* 171: 323–326, 1989.
7. Mahfouz A-E, Hamm B, Taupitz M, Wolf K-J. Hypervascular liver lesions: differentiation of focal nodular hyperplasia from malignant tumors with dynamic gadolinium-enhanced MR imaging. *Radiology* 186: 133–138, 1993.
8. Wanless IR, Mawdsley C, Adams R. On the pathogenesis of focal nodular hyperplasia of the liver. *Hepatology* 5: 1194–1200, 1985.
9. Rogers JV, Mack LA, Freeny PC, Johnson ML, Sones PJ. Hepatic focal nodular hyperplasia: angiography, CT, sonography, and scintigraphy. *AJR* 137: 983–990, 1981.
10. Takayasu K, Muramatsu Y, Moriyasu N, Yamazaki S, Takayama T, Hirohashi S, et al. Focal nodular hyperplasia of the liver: arterial angio-CT and microangiography. *J Comp Assist Tomogr* 16: 212–215, 1992.
11. Kudo M, Tomita S, Minowa K, Tochio H, Shimada K, Mimura J, et al. Color Doppler flow imaging of hepatic focal nodular hyperplasia. *J Ultrasound Med* 11: 553–557, 1992.
12. Yamamoto H, Yamanaka T, Yoshida Y, Miyata M. Detection of focal nodular hyperplasia of the liver with color Doppler ultrasonography. *Gastroenterol Jpn* 28: 424–430, 1993.
13. Kerlin P, Davis GL, McGill DB, Weiland LH, Adson MA, Sheedy II PF. Hepatic adenoma and focal nodular hyperplasia: clinical, pathologic, and radiologic features. *Gastroenterology* 84: 994–1002, 1983.
14. Cherqui D, Rahmouni A, Charlotte F, Boulahdour H, Métreau J-M, Meignan M. Management of focal nodular hyperplasia and hepatocellular adenoma in young women: a series of 41 patients with clinical, radiological, and pathological correlations. *Hepatology* 22: 1674–1681, 1995.
15. Stadalnik RC, Vera DR, Woodle ES, Trudeau WL, Porter BA, Ward RE, et al. Technetium-99m NGA functional hepatic imaging: preliminary clinical experience. *J Nucl Med* 26: 1233–1242, 1985.
16. Kurtaran A, Li S-R, Raderer M, Leimer M, Müller C, Pidlich J, et al. Technetium-99m-galactosyl-neoglycoalbumin combined with iodine-123-try-(A14)-insulin visualizes human hepatocellular carcinomas. *J Nucl Med* 36: 1875–1881, 1995.
17. Sawamura T, Nakada H, Hazama H, Shiozaki Y, Sameshima Y, Tashiro Y. Hyperasialoglycoproteinemia in patients with chronic liver diseases and/or liver cell carcinoma. *Gastroenterology* 87: 1217–1221, 1984.
18. Saito K, Koizumi K, Abe K, Goto Y, Seki T. Potential for quantitative diagnosis of tumor and tumors lesions in the liver with Tc-99m-GSA SPECT—Correlation with pathological evaluation and MRI findings—. *Ann Nucl Med* 12: 275–280, 1998.
19. Hyodo I, Mizuno M, Yamada G, Tsuji T. Distribution of asialoglycoprotein receptor in human hepatocellular carcinoma. *Liver* 13: 80–85, 1993.
20. Kutaran A, Müller C, Novacek G, Kaserer K, Mentes M, Raderer M, et al. Distinction between hepatic focal nodular hyperplasia and malignant liver lesions using technetium-99m-galactosyl-neoglycoalbumin. *J Nucl Med* 38: 1912–1915, 1997.
21. Strauss LG, Conti PS. The applications of PET in clinical oncology. *J Nucl Med* 32: 623–648, 1991.
22. Okazumi S, Isono K, Enomoto K, Kikuchi T, Ozaki M, Yamamoto H, et al. Evaluation of liver tumors using fluorine-18-fluorodeoxyglucose PET: characterization of tumor and assessment of effect of treatment. *J Nucl Med* 33: 333–339, 1992.
23. Torizuka T, Tamaki N, Inokuma T, Magata Y, Sasayama S, Yonekura Y, et al. *In vivo* assessment of glucose metabolism in hepatocellular carcinoma with FDG-PET. *J Nucl Med* 36: 1811–1817, 1995.